Unobtrusive and Robust Human Identification Using COTS RFID

Qian Zhang[a,*], Run Zhao[b], Dong Li[a], Dong Wang[a,*]

[a] *School of Software, Shanghai Jiao Tong University*
[b] *Computer Science Department, Shanghai Jiao Tong University*

Abstract

Human identification is a prerequisite for many personalized services in smart spaces. This paper presents RFree-ID, the first unobtrusive RFID-based human identification system irrespective of walking cofactors (*e.g.* carrying a backpack or a briefcase). The key insight is that the RFID reader and tags can serve as a radio gate, and the walking-induced RF signal fluctuations from tags are capable of perceiving different walking patterns when people cross this gate. More importantly, spatially separated tags can provide abundant temporal and spatial information for amplifying discrepancies among people and minifying the influence of walking cofactors. Therefore, after collecting phase fluctuations received from RFID tags, RFree-ID identifies people by using a sequence of signal processing techniques and a well-designed matching algorithm. The system is implemented on COTS RFID devices, and extensive experimental evaluation under various conditions validates the high reliability and robustness of our system.

Keywords: human identification, COTS RFID, spatial diversity, walking cofactors

1. Introduction

1.1. Motivation and Proposed Approach

Radio-based human sensing techniques have drawn significant attention in recent years. Due to the merits of unobtrusiveness and privacy protection, they have fostered a wide range of innovative applications such as localization [1], activity recognition [2][3], and even vital signs monitoring [4], all of which offer great potential to enhance the quality of our work and life. However, without knowing the identities of individuals, many of these applications would largely reduce the user experience and even worse become infeasible in realistic scenarios. For example, if activity recognition systems cannot identify someone

*Corresponding author
Email addresses: qwert3472@sjtu.edu.com (Qian Zhang), wangdong@sjtu.edu.com (Dong Wang)

who is walking into a room, they fail to further provide him/her with personalized services like TV program recommendations. On the contrary, a system enabling unobtrusive and reliable human identification will obviously facilitate the applications of radio-based sensing.

Existing radio-based human identification systems [5][6] have proven that gait can be regarded as a credible and discriminative indicator for different people. These systems leverage the detailed Channel State Information (CSI) of WiFi signals to profile unique walking patterns. However, it is worth noting that walking patterns are restricted by various walking cofactors, such as appearance changes caused by carrying a backpack or a briefcase and inconsistent walking paths. And these pioneer works put strong constraints on the walking pattern consistency between training processes and identifying processes. More specifically, walking cofactors must remain identical for one specific person among all processes due to the sensitivity of wireless channel metrics to multipath changes. Despite the fact that WiFi signals can provide rich frequency diversity, fusing the CSI measurements on multiple subcarriers still cannot effectively handle the variations of walking cofactors [6]. The main problem is that all these subcarriers share the same propagation paths, resulting in indistinguishable discrepancies among them. One possible solution is to offer spatial diversity by deploying several pairs of transmitters and receivers. Since signals from each pair possess their own propagation paths, they would experience utterly different distortions when people walk. Motivated by this, we turn our attention to the passive RFID technology which can accomplish this goal by simply attaching an array of inexpensive tags in the space. Apparently, the impacts exerted by walking cofactors vary considerably across all tags, opening up a new opportunity for gait-based human identification.

In this paper, we devise RFree-ID, a first-of-its-kind device-free human identification system with Commercial Off-The-Shelf (COTS) RFID products [7]. Our vision is that RFree-ID can reliably discern people irrespective of walking cofactors when they walk along straight walkways (doors, corridors, etc.). The key insight is that, the RFID reader and an array of tags which are on either side of the walkway can serve as a radio gate, and when people cross the gate, the fine-grained phase information from RF signals is capable of perceiving walking patterns. More importantly, phase profiles from spatially separated tags can offer abundant temporal and spatial information, which can definitely boost the precise human identification.

1.2. Technical Challenges and Solutions

Although the rationale behind sounds quite simple, some rigorous challenges require to be addressed. First of all, even though there exists gait diversity in people, the difference exhibited by phase profiles can be quite small among some people, making them hard to be distinguished. In addition, it is extremely difficult to guarantee that walking patterns are always identical for one person in real scenarios because any variations of walking cofactors will make a big difference. The spatial diversity provided by RFID tags holds potential to deal with the variations, but how to incorporate the information across multiple tags

is non-trivial. Although many sophisticated RFID systems for activity recognition have emerged recently, e.g. IDsense [8], ShopMiner [9] and FEMO [10], they mainly focus on recognizing human object interactions by perceiving movements of RFID tags attached on objects. Some other works [11][12] recognize human activities by perceiving multipath changes. They also deploy multiple tags in the environment to provide spatial diversity. However, they assign equal weight to each tag, greatly limiting the potential of multiple tags and making their systems vulnerable to cofactors changes [12]. Moreover, the discrepancies exhibited in phase profiles among walking people are far less than those among different activities [13], and thus we need a more elaborate algorithm to capture these discrepancies.

In this paper, we deploy an array of separated tags in the space and explore the full potential of the spatial diversity in human identification. On one hand, when different people walk through the radio gate composed of the reader antenna and tags, walking diversity can be accurately captured by this tag array. Although, for some tags, phase fluctuations are almost the same from one person to another, there are usually some other tags fluctuating divergently among people. And RFree-ID attempts to discern people by magnifying the influence of those tags with high distinguishability. On the other hand, this tag array can also mitigate the effect of various walking cofactors. When a person walks with different cofactors, there may exist some tags whose phase fluctuations remain almost unchanged although those for other tags distort dramatically. Thus, RFree-ID plans to relax the restriction of walking pattern consistency by suppressing the impact of those most distorted tags. To maximize the benefits provided by spatial diversity, RFree-ID first quantifies the distinguishability and distortion for each tag, and then proposes a Weighted Multi-dimensional Dynamic Time Warping (WMD-DTW) algorithm to accurately identify people irrespective of walking cofactors.

1.3. Applicability

Recent advances in RFID, such as RFID light bulbs [14] which integrate the reader into a smart lamp, prospectively facilitate the deployment of our system, especially in home settings. Furthermore, compared to WiFi-based systems which require people to walk along a line for about 5m and are susceptible to the changes of walking cofactors, our system can effectively handle these variations while people just need to cross the radio gate. Hence, we envision that RFree-ID does apply to a wide range of applications. For example, we can deploy our system on the door frame of each room in a house to identify the person crossing the doors, enabling personalized room-level applications and behavior analysis. As for scenarios where RFID systems have already been deployed, like warehouses and offices, we can reuse existing infrastructures to identify and track employees unobtrusively. In this paper, we prototype two example applications based on RFree-ID, i.e. a corporate library management system and an office room-level tracking system. In the first application, the system enables automatic user-book pairing when people walk into or out of the library with books. In the second application, as office buildings are usually

organized into rooms with distinct functionalities (also true for home or industrial environments), employees' room-level location information can reveal their daily activities, which provides precious information for employees to improve their work habits (e.g. avoiding long-term sedentary work). We perform in-situ experiments for both systems and the promising performance further confirms the practical value of RFree-ID.

1.4. Contributions

In summary, our main contributions are as follows:

- To the best of our knowledge, this is the first attempt to design an unobtrusive human identification system based on COTS RFID devices. We have demonstrated that the walking-induced phase profiles are abundant enough to capture walking patterns for human identification.
- We conduct extensive experiments to validate the potential of the spatial diversity provided by spatially separated RFID tags. Based on these experiments, we devise a distinguishability estimator and a distortion estimator to quantitatively appraise distinguishability and distortion for each tag, respectively, and then apply a well-designed WMD-DTW algorithm to accurately discern people by amplifying discrepancies among them and minifying the influence of walking cofactors.
- We implement RFree-ID and comprehensively evaluate the performance in a typical office building under various conditions. Experimental results show that RFree-ID can achieve 97% identification accuracy with a group of 10 people under ideal situations where walking cofactors remain unchanged, and 93.5% in a real world scenario where people can freely change their walking cofactors.
- To illuminate practicability of our system, we have designed and developed two prototype applications on top of RFree-ID. Our workplace library management system can pair the book with the person borrowing it with 96.5% accuracy. In the room-level tracking scenarios, by integrating the tracking techniques with our identification algorithm, we can enable 95.4% localization accuracy.

The rest of the paper is organized as follows. We review the related works in Section II and present an overview of the system in Section III. Then we present the detailed design of RFree-ID in Section IV and the system implementation and performance evaluation in Section V. We also present two prototype applications in Section VI. Finally, we present discussion and conclusion of this paper in Section VII.

2. Related Work

This section reviews the related literature in RFID-based sensing and gait identification techniques.

2.1. RFID-based sensing

RFID is normally considered as an enabling tool for automatic identification of objects. Amazingly, recent research has shown that the physical RF signal between RFID readers and tags can be a powerful sensing modality for many applications. Some works [15][16][17] leverage the signal phase to locate RFID tags within high precision. Much attention has also been paid on activity and gesture recognition, like shopping behavior mining [9], exercise monitoring [10], falling detection [11][12] and fluid intake recognition [18]. IDsense [8] detects human object interactions by perceiving movements of tags attached on everyday objects. Grfid [19] adopts a multiple-tag method to realize a robust gesture recognition system. PaperID [20] and Rio [21] turn RFID tags into input devices by sensing signal changes. Different from the state-of-the-art systems mentioned above, RFree-ID aims to unobtrusively identify people by measuring gait diversity exhibited in low-level RF phase information. We construct more distinctive features and matching algorithms for human identification with spatially separated tags.

2.2. Gait-based human identification

Gait-based human identification aims to discriminate individuals by the way they walk. Unlike other biometrics, gait can be captured at a distance and without requiring the extra cooperation from people. Camera-based approaches [22, 23] use spatial-temporal silhouette analysis based on computer vision to perform identification. Such methods highly depend on lighting conditions and require line-of-sight as well as suffer from privacy concerns. Even some systems are designed not to report images, privacy leaks can still happen if the camera systems are hacked. Wearable sensor-based methods [24][25] employ inertial sensors embedded in mobile devices to capture gait signature. Ambient sensor-based systems provide a non-intrusive way by exploiting the ambient information including audio [26], pressure [27] and floor vibration [28] produced by walking while their further applications may be hindered by the requirement of specialized devices and high deployment cost.

Since human motions will cause multipath changes of wireless signals, researchers have also utilized wireless signals to identify people. Authors in [29] extract micro-Doppler signature based on radar techniques to characterize the gait pattern. RF-Capture [30] leverages the captured human figure via FMCW radar to deliver human identification and gesture recognition. A more promising alternative is to employ the fine-grained Channel State Information (CSI) which has already been exposed by commodity WiFi cards for human identification [5][6][13][31]. However, these methods put strong constraints on walking cofactors consistency, which does not always hold in practice. Recent work Rapid [32] makes an exploration to handle walking path inconsistency, but it still does not consider other common walking cofactors in real-life such as carrying a backpack. In comparison to these WiFi-based methods, RFree-ID constructs more distinguishable walking-induced phase profiles and is robust to various confounding factors. Furthermore, RFree-ID only needs people to cross the radio gate, which is deployable to a wider range of applications.

3. RFree-ID Overview

In this section, we first briefly analyze the principle of gait-based human identification with COTS RFID devices. Next, two sets of preliminary experiments are performed to elaborate on the benefits and necessities of spatial diversity provided by multiple tags. Finally, we provide an overview of our system.

3.1. Principle

Present COTS RFID readers, such as Impinj Speedway in our implementation, can report the low-level backscatter signal characteristics such as RSSI, phase and Doppler shifts [33]. Our system exploits the phase information for human identification as it exhibits a more reliable and fine-grained indicator of multipath changes than other metrics [19].

In most practical RFID setups, the integrated signal received by the reader is the superposition of signals from the Line of Sight (LOS) path and many other reflected paths due to the multipath effect. When a person walks through a radio gate composed of a reader and a tag, some propagation paths remain invariant (static paths) while others change with human movements (dynamic paths). The received signal of the reader can hence be presented by:

$$s(t) = s_{\mathrm{s}}(t) + s_d(t) = s_s(t) + \sum_{k=1}^{N} a_k(t) e^{-j2\pi f \tau_k} \tag{1}$$

where $s_s(t)$ and $s_d(t)$ denote the sum of time-varying signals from static paths and dynamic paths, respectively. $a_k(t)$ is the complex valued representation of attenuation and the initial phase offset of the k^{th} dynamic path. $e^{-j2\pi f \tau_k}$ is the phase shift on this path with a propagation delay of τ_k and f is the carrier frequency. Then the received signal phase $\angle s(t)$ can be further derived as:

$$\angle s(t) = \arctan \frac{|s_s(t)| \sin \angle s_s(t) + |s_d(t)| \sin \angle s_d(t)}{|s_s(t)| \cos \angle s_s(t) + |s_d(t)| \cos \angle s_d(t)} \tag{2}$$

where $|\cdot|$ and $\angle\cdot$ represent the amplitude and phase of the corresponding signal, respectively.

Two significant inferences can be drawn from Eq. (1) and Eq. (2). In order to facilitate the understanding, we ask a volunteer to cross the gate (Fig. 1). The extracted phase profiles are plot in Fig. 2. As the DC parts of the profiles have been removed, a phase shift of $3rad$ means that the phase is $3rad$ larger than that without human motions.

The first inference is that the received phase $\angle s(t)$ is highly related to signals from walking-induced dynamic paths. Eq. (1) indicates that changes in the length of any signal propagation path lead to corresponding phase changes of the RF signal on this path. In theory, a change of half a wavelength generates a πrad phase shift. When the volunteer is approaching the LOS path between the reader and tags, the length of the body-reflected path will gradually decrease, resulting in a periodic change ($0 \sim 2\pi$) in the signal phase of this path. In addition, the

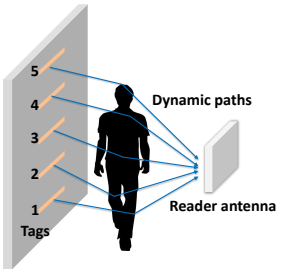

Figure 1: The setup of RFree-ID

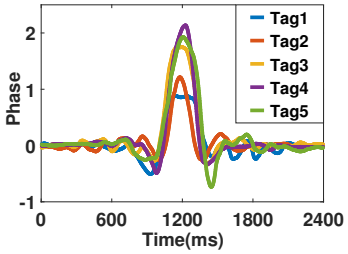

Figure 2: Profiles of spatially separated tags

signal amplitude will also become larger owing to a shorter path. Accordingly, we can infer from Eq. (2) that the combined signal phase $\angle s(t)$, which is a consequence of dynamic body-reflected paths and static paths, will experience a gradually increasing amplitude of oscillation. Similarly, $\angle s(t)$ will experience a gradually decreasing amplitude of oscillation when the person is moving away from the LOS path. It can be observed that the result shown in Fig. 2 is very consistent with our analysis. Since there exists gait diversity among people, walking-induced dynamic signals must be different from one person to another and thereby these phase fluctuations can be regarded as a unique indicator for a specific person.

The second inference is that as walking-induced signals from spatially separated tags travel along divergent paths, phase fluctuations will also be different, which can be verified by Fig. 2. This inspires us to construct more distinguishable features for each individual with rich spatial diversity provided by multiple tags.

It is noteworthy that the tag can still be read by the reader when the LOS path is blocked due to the diffraction and the multipath propagation of the RF signal, so the corresponding signal phase will have a gradual change instead of a jump [34]. Moreover, the phase profiles fluctuate more prominently when people are crossing or near the LOS path. During this short period, the fluctuation is mainly generated by human bodies' forward motions rather than their walking steps. Our extensive experiments show that even for tags close to the ground, the effect of the steps is negligible, indicating that our system is resilient to the number of walking steps.

3.2. Spatial Diversity

As shown in Fig. 1, in order to generate spatial diversity for RFree-ID, tags are spatially distributed in the vertical direction, numbering 1 to 5 from the bottom to the top. Obviously, the specific deployment of tags such as tag numbers and tag intervals, are able to have a great influence on the system performance, which will be detailedly discussed in Section V. And we perform two sets of preliminary experiments to illustrate the benefits and necessities of spatial diversity.

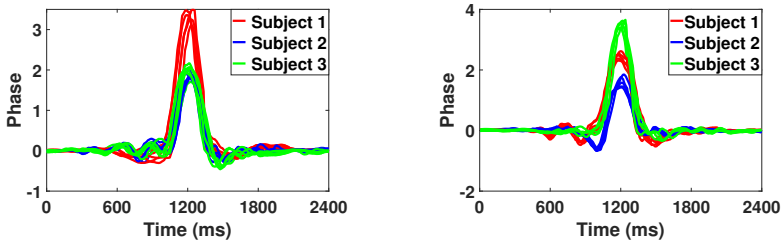

(a) Tag 3 for Subject 1,2 and 3 (b) Tag 5 for Subject 1,2 and 3

Figure 3: Phase profiles of different people

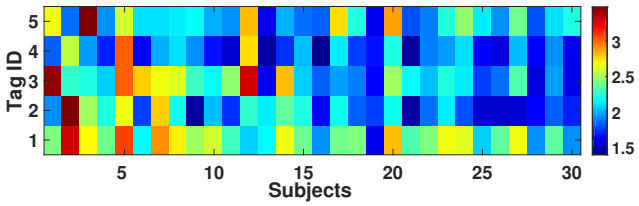

Figure 4: The maximum values of the phase profiles from 30 subjects

Compared with a single tag, intuitively, multiple tags can capture the gait diversity engendered by different individuals in a more precise way. In order to corroborate this intuition, three subjects are asked to walk along a straight line between a reader and a tag array in a corridor separately (5 tests each one). The processed phase profiles of tag 3 and tag 5 for these three subjects are illustrated in Fig. 3(a) and Fig. 3(b), respectively. We depict phase profiles of each test on the figures for the sake of demonstrating their stability and repeatability. As shown in Fig. 3(a), although phase profiles for Subject 1 can be apparently separated from those for Subject 2 and 3, the discrepancy between Subject 2 and 3 is so small that they cannot be differentiated by phase profiles only from this tag. However, as we can observe from Fig. 3(b), the phase profiles of these three subjects from tag 5 are discriminate enough to tell them apart. For a better illustration, we collect the phase profiles of 30 subjects and show the maximum values of these profiles in Fig. 4. From the figure, we can see that even though the maximum values of a certain tag are close among some people, it is hard to find any two people whose maximums of phase profiles are close across all tags. Apparently, the maximum as well as other standard time-frequency features cannot completely characterize the unique walking patterns, but Fig. 4 still shows the powerful potential provided by spatially separated tags on boosting the walking pattern distinguishability.

As mentioned before, superior to WiFi based human identification systems, RFree-ID has the ability to mitigate the effect of walking cofactors. In order to expound how it works, one subject is invited to walk with and without a

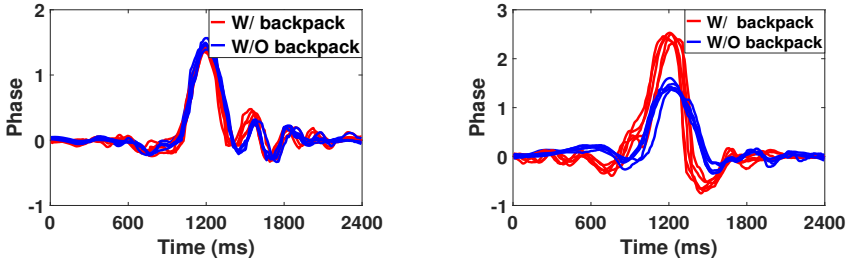

(a) Tag 1 for Subject 4 (b) Tag 3 for Subject 4

Figure 5: Phase profiles with and without carrying a backpack

backpack. As shown in Fig. 5(a), the phase profiles of tag 1 under these two conditions are almost identical, whereas those of tag 3 in Fig. 5(b) are heavily distorted by the change of walking cofactors, which indicates that the distortion caused by walking cofactors can be effortlessly detected and further diminished by our multiple-tag system.

From these experiments, we can draw an significant conclusion that it would prospectively improve the distinguishability among people as well as the robustness to the changes of walking cofactors by employing phase profiles across multiple spatially separated tags.

3.3. System Overview

RFree-ID consists of a RFID reader and an array of spatially separated RFID tags, which can be deployed on either side of a corridor or an entrance. Fig. 6 shows a general overview of our system, containing 4 modules in total. After being filtered by the *Signal Preprocessing* module, phase measurements are passed through the *Walking Detection* module to extract the data that contains walking events. Then extracted phase profiles are further purified with *Profile Extraction* and *Wavelet Denoising*. We also estimate the walking direction by comparing the LOS time of the tag array and the direction tag which is on the left/right of the array. Finally, processed phase profiles are fed into the core component called the *Human Identification* module. To amplify the discrepancies among people and mitigate the impact of walking cofactors, this module estimates the distinguishability and distortion for each tag, and then applies *Weighted Multi-Dimensional Dynamic Time Warping (WMD-DTW)* to compute the similarity of two walking profiles. RFree-ID determines the identity of a person by searching the one in the walking profile library which has the highest as well as sufficient similarity with the testing profile.

4. System Design

This section details four modules of RFree-ID, including *signal preprocessing, walking detection, feature extraction and human identification.*

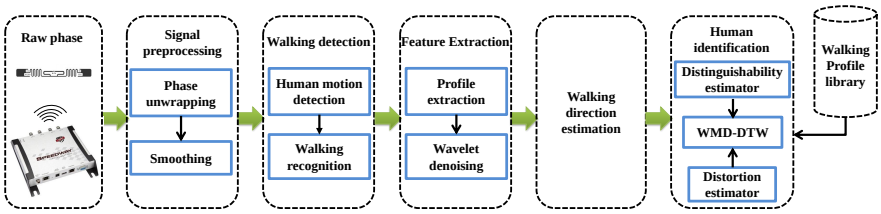

Figure 6: The overview of RFree-ID

4.1. Signal Preprocessing

Phase Unwrapping: The first step to process the raw phase measurements is phase unwrapping. The reason is that the signal phase reported by the reader is a periodic function ranging from 0 to 2π, termed as wrapped phase [19]. We adopt the method in [9] to unwrap the phase values, which assumes that the absolute difference of two adjacent reading phase values is smaller than π. This is reasonable given that the frequency of human body moving is well below than that of the reader interrogation.

Smoothing: After phase unwrapping, RFree-ID applies the Hampel identifier and a weighted moving average filter to smooth the data. Then, the system removes the Direct Current (DC) component of phase stream by subtracting the constant offset which can be calculated via a long-term averaging over the stream. At last, since tags reply unevenly spaced in time domain, we adopt linear interpolation with $10ms$ apart between consecutive values to process the phase stream.

4.2. Walking Detection

As shown in Fig. 6, the walking detection module consists of two steps. The first one is to detect the occurrence of human motions and extract the corresponding phase data. And the second one is to figure out whether the motion is walking based on the extracted data from the previous step.

Motion Detection: Intuitively, phase values remain relatively stable with no presence of human motions while noticeably fluctuate otherwise. This inspires us to employ the Kullback-Leibler divergence (KL-divergence) to detect potential human motions [10]. We first segment the phase stream into frames of $1s$ with 50% overlap and then calculate the KL-divergence for each two consecutive frames. In the absence of human motions, the value of KL-divergence is small due to the stability of phase values. Conversely, the values become large when a moving human appears. Thus, we can single out human motion data by checking the value of KL-divergence. To avoid missing meaningful phase data, we extract the motion data aggressively which will be further refined in the next section.

Walking Recognition: The goal of this stage is to separate walk from other human motions. It is not hard to understand that different human activities exhibit distinguishable pattern in both time and frequency domain. And a set of

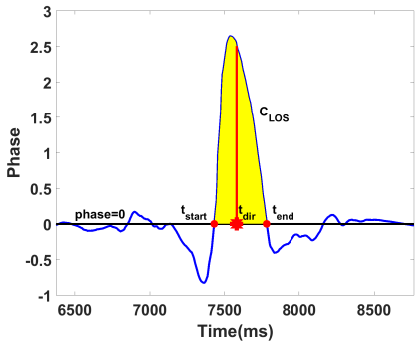

Figure 7: Walking direction estimation

light weight features for each tag are computed from the extracted motion data to characterize different activities, including 7 time-domain features, *i.e.* mean, max, min, skewness, kurtosis, variance, mean crossing rate and 3 frequency-domain features, *i.e.* spectral entropy, band energy, the largest FFT peaks. Afterwards, a decision tree classifier is adopted using these features to determine whether the human motion is walking.

4.3. Feature Extraction

Once the system detects the occurrence of walking, the human identification scheme will be triggered. However, the extracted data are still coarse-grained and may contain parts of meaningless phase samples. Hence, this step realizes a more fine-grained extraction. As mentioned in Section 3.1, the amplitude of phase fluctuation will reach the maximum when the person is crossing the LOS path. Based on this insight, RFree-ID segments the extracted data into several frames ($0.1s$ with 50% overlap) and finds the frame with the maximum average energy. The mid-point time of this frame is considered as the moment that the person is crossing the LOS path, denoted as t_{mid}. The duration T_p of the walking phase profiles is set to $2.4s$ via the trial-and-error method. Then the phase data in $[t_{mid} - \frac{T_p}{2}, t_{mid} + \frac{T_p}{2}]$ is extracted and delivered to a wavelet filter. We apply 5-level 'db4' Discrete Wavelet Transform (DWT) to denoise these profiles [35]. Finally, RFree-ID constructs the walking profile for each individual with the denoised phase profiles from spatially separated tags.

4.4. Walking Direction Estimation

As the signal phase is sensitive to multipath changes, the perceived phase profiles will change significantly when people walk through the portal in the opposite direction. Therefore, we need to match the testing profile with training profiles in both directions to identify the individual as well as determine his/her walking direction. On the other hand, if the direction can be obtained in advance, the computational load in the matching phase will obviously decrease. For this, we deploy an additional tag on the left/right of the tag array as the

direction tag. A straightforward idea is to estimate the direction based on t_{mid} (Section 4.3) of the direction tag and the tag array, which is error-prone when their horizontal space is small. Here, we propose a more robust method to estimate the walking direction. When an individual is crossing the LOS path, the phase profile of each tag will first increase and then decrease. We denote the curve in this interval as C_{LOS} (Fig. 7), and calculate the area of the region surrounded by C_{LOS} and the line $phase = 0$, which is $\int_{t_{start}}^{t_{end}} C_{LOS}$. t_{start} and t_{end} are the corresponding time of the intersection points of C_{LOS} and $phase = 0$. Then we find t_{dir} satisfying:

$$\int_{t_{start}}^{t_{dir}} C_{LOS} = \frac{1}{2} \int_{t_{start}}^{t_{end}} C_{LOS} \tag{3}$$

We determine the walking direction by comparing t_{dir} of the direction tag and the tag next to it in the tag array. If t_{dir} of the direction tag is smaller, the direction is estimated as from the direction tag to the tag array, and vice versa.

4.5. Human Identification

We adopt *Dynamic Time Warping* (DTW) to compute the similarity between two phase profiles considering that people may cross the gate at different speeds. We make two improvements on traditional DTW to speed up computation and prevent unlimited stretch [36]. First, when generating the cost matrix(the element $c_{i,j}$ are the absolute difference of p_i and q_j from the two sequences), RFree-ID applies a window constraint which means only those elements that i and j don't differ too much are calculated (≤ 30 in our system). The rationale behind this is that the elements in the optimal warping path are highly likely located in the region around the diagonal line of the matrix when taking our elaborate *profile extraction* method into account. This window constraint can not only speed up DTW computation but also prevent pathological alignments.

In addition, traditional DTW just considers the difference of p_i and q_j while neglecting the difference of i and j, which will easily lead to a small DTW distance when the two profiles have similar amplitudes but different shapes. An additional cost, called stretch cost, is introduced to deal with the effect of unlimited stretching. Hence, the DTW distance with stretch cost is denoted as:

$$DTW(P, Q) = \sum_{i,j} \left(|p_i - q_j| + \gamma \times |i - j| \right) \tag{4}$$

where i and j are the pair of the optimal warpping path. $\gamma \times |i-j|$ is the stretch cost and γ is the scale factor. We should choose a small value for γ, because a large one will degrade the efficiency of DTW for stretching alignment. Also, the value of $|p_i - q_j|$ is usually much smaller than that of $|i - j|$. Considering these factors, we empirically set γ as 0.02 in our system.

As the walking profile of each individual consists of multiple phase profiles from spatially separated tags, *Multi-Dimensional Dynamic Time Warping* (MD-

DTW) [35] easily comes to mind, which can be formulated as follows:

$$d(P,Q) = \sum_{i=1}^{N} DTW(P_i, Q_i) \tag{5}$$

where P_i and Q_i are the profiles from the i_{th} tag, and N is the number of the tags. However, this naive method considers that all tags participate equally for human identification, limiting the full advantage of spatial diversity provided by multiple tags. As mentioned before, there are two benefits obtained from spatial diversity. The first one is that there exist some tags whose phase profiles fluctuate divergently among people, which means they exhibit more distinguishability than other tags. And the second one is that phase profiles from some tags almost remain invariant with different walking cofactors, which indicates that they experience less distortion than other tags. Undeniably, higher weights should be assigned to those two kinds of tags. RFree-ID enables the weighting mechanism via two estimators, i.e., distinguishability estimator and distortion estimator, which are performed in the training process and identifying process, respectively.

Distinguishability Estimator: The distinguishability estimation for each tag is performed in the training process. Given the trained profiles of the target group, RFree-ID calculates two types of DTW distance for each tag, the intra-class distance and the inter-class distance. The former is the average of the DTW distance between any two phase profiles from the same person, and the latter is the average of that from two different persons. It is intuitive that tag i is more discriminative when it has a smaller intra-class distance and a larger inter-class distance. Based on this insight, we determine the discriminative weight of each tag as :

$$\alpha_i = \frac{\overline{DTW}(Q_i^{k,m}, Q_i^{l,n})_{(k \neq l)}}{\overline{DTW}(Q_i^{k,m}, Q_i^{k,n})_{(m \neq n)}} \tag{6}$$

where $Q_i^{k,m}$ is the m_{th} profile of person k in the profile library. After normalization, we get the global discriminative weight of each tag. Besides, we also calculate the local discriminative weight of each tag for any two persons in the group.

Distortion Estimator: In the identifying process, given the testing profile of tag i, P_i, RFree-ID first calculates the DTW distance between P_i and every profiles in the trained library. Then the average of the k_{th} person's DTW distance with respect to tag i can be represented by $\overline{DTW}_k(P_i, Q_i^{k,m})$. We calculate this value for each person and denote the minimum as $min(\overline{DTW}_k(P_i, Q_i^{k,m}))$. We also have the intra-class distance for tag i. The ratio of them is:

$$Ra_i = \frac{min(\overline{DTW}_k(P_i, Q_i^{k,m}))}{\overline{DTW}(Q_i^{k,m}, Q_i^{k,n})_{(m \neq n)}} \tag{7}$$

The intuition underlying our distortion estimation mechanism is as follows. If the testing profile of tag i is distorted slightly, the $min(\overline{DTW}_k)$, which usually equals to the average DTW distance between the testing profile and the

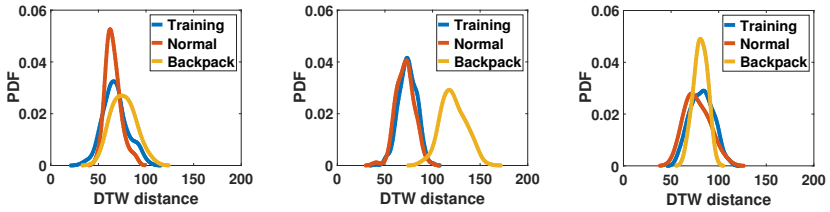

(a) (b) (c)

Figure 8: PDF of DTW distance (a) tag 1; (b) tag 3; (c) tag 5

individual's corresponding training profiles, will yield a small value, otherwise, the value will achieve large. Therefore, higher Ra_i indicates the profile of this tag is less reliable in human identification, in other words, Ra_i can be used to quantify the distortion of tag i. We illustrate this idea in Fig. 8. We select the profiles of Subject k with respect to tag 1, tag 3 and tag 5. The blue line is the DTW distance PDF (probability density function) of Subject k's any two profiles in the training library. For comparative analysis, we ask Subject k to walk normally (just as in training phase) once again and compute the DTW distance between the walking profile collected this time and his profiles in the library. The red line is the PDF. It can be observed that the DTW distance distribution of three tags changes little. Then we ask Subject k to walk carrying a backpack and the yellow line is the corresponding PDF. We can see that the DTW distance distribution of tag 3 in this experiment is totally different from training data while that of tag 1 and tag 5 remain stable, indicating that the profile of tag 3 distorted much more seriously. It can be observed that the value of Ra_i can well quantify this distortion. We assign a dynamic weight for tag i according to the distortion estimation:

$$\beta_i = \frac{\frac{1}{Ra_i}}{\sum_{i=1}^{N} \frac{1}{Ra_i}} \tag{8}$$

WMD-DTW: After the weight of each tag is calculated, we get the Weighted MD-DTW distance:

$$d(P,Q) = \sum_{i=1}^{M} \alpha_i \times \beta_i \times DTW(P_i, Q_i) \tag{9}$$

where α_i and β_i are the global discriminative weight and the dynamic weight of tag i, respectively. Given one testing walking profile, RFree-ID calculates the similarity between it and the kth person in the target group as follows: First, the system calculates the WMD-DTW distance between this profile and all the labeled walking profiles of person k in the profile library. Then, the system selects the top L smallest distance, sorted as $d_{k,1} < d_{k,2} < \cdots < d_{k,L}$, and the final similarity between the testing profile P and person k is quantified via a

weighted average scheme:

$$d(P,k) = \sum_{l=1}^{L} \frac{L+1-l}{L} \times d_{k,l} \tag{10}$$

RFree-ID calculates this distance for all the persons in the group and selects the two people corresponding to the top-2 smallest distance. Afterwards, the system selects the two people corresponding to the top-2 smallest distance and recalculates the similarity using the square of these two candidates' local discriminative weights instead of α_i in Eq. (9). The person with the smaller distance is determined as the final result.

Note that if the smallest distance is larger than a threshold, it is highly likely that the testing profile belongs to a stranger. This paper primarily focuses on the identification of people who has enrolled his/her walking profile in the training library, and we leave stranger detection to our future work.

5. Implementation and Evaluation

5.1. Implementation

Devices and Deployment: We implement RFree-ID using off-the-shelf RFID devices. The reader is Impinj Speedway R420 reader equipped with a directional antenna (Laird S9028 with $9dBi$ gain). The tags are ALN-9740. We evaluate the performance of RFree-ID in a typical office building, as Fig. 9 shows. The reader and tags are deployed on either side of a corridor. The horizontal distance between them is $2m$. The reader antenna is $0.8m$ high, and the tags are uniformly distributed in the vertical direction from $0.4m$ to $1.8m$.

Data Collection: We collect training and testing data from 30 volunteers for evaluation. These volunteers are 22 male and 8 female university students with the age ranging from 21 to 25. We also record their weights (male: $56 \sim 74kg$; female: $46 \sim 52kg$) and heights (male: $168 \sim 184cm$; female: $160 \sim 167cm$). To construct the walking profile library, we instruct the subjects to walk normally (carrying no objects) along a predefined path (Path1 in Fig. 9) for 50 times. As the walking profile will change obviously when people walk in the opposite direction, we collect profiles in both directions.

5.2. Walking Detection Accuracy

To evaluate the performance of our walking detection scheme, we ask volunteers to perform non-walking activities besides walking, i.e. walking around the sensing area, standing in the sensing area making phone calls, walking towards portal and then walking back, passing by the portal, sitting down and standing up. Here, the sensing area refers to the area where people inside can have pronounced effects on the received signal. Table 1 shows the confusion matrix of the detection results. As the fact that the confined space only allows limited human activities, our scheme yields a nearly perfect accuracy.

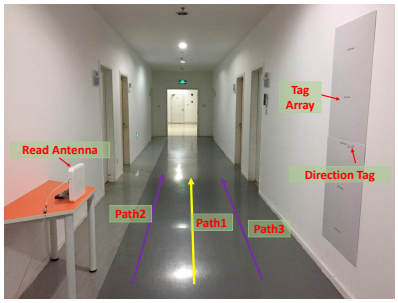

Figure 9: Experimental setup

classified as	walking	non-walking
walking	0.997	0.003
non-walking	0.004	0.996

Table 1: Confusion matrix of walking detection when there are 5 tags

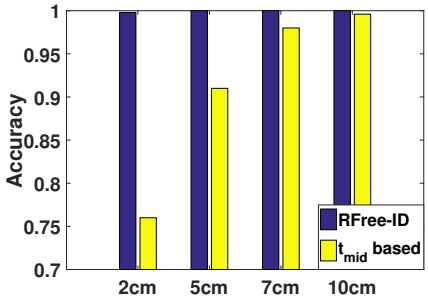

Figure 10: Walking Direction Estimation

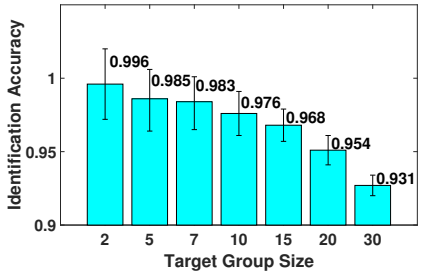

Figure 11: Identification Accuracy VS Target Size

5.3. System Performance in Direction Estimation

In this section, we measure the performance of our direction estimation method and compare it with t_{mid} based method. We vary the horizontal interval between the direction tag and the tag array from $2cm$ to $10cm$. Fig. 10 illustrates the accuracy of these two methods. We can see that our method can still identify the direction with 99.8% accuracy when the horizontal interval is only $2cm$, far more reliable than the other method. Given the space limitations, we choose $2cm$ as the interval between the direction tag and the tag array.

5.4. System Performance in Normal Walking

In this section, we evaluate the performance of RFree-ID when people walk normally along a predefined path. We use the data in the profile library as testing profiles and acquire the identification accuracy of each subject via $K_f - fold$ cross validation. The training set size and tag number is 20 and 5 by default, respectively, and we will investigate the impact of these two parameters in Section 5.9 and 5.10. Fig. 11 shows the performance of RFree-ID under different target group sizes. We observe that the identification accuracy of RFree-ID decreases with the group size increasing. In particular, the accuracy

Code	Walking Cofactors	Code	Walking Cofactors
a	carrying a backpack	d	clothes
b	making a phone call	e	another walking path
c	carrying a laptop	f	environmental change

Table 2: Walking Cofactors

of RFree-ID yields 99.6% when there are only two subjects in the group, and decreases to 93.1% with the group size of 30. When the size is 10, the average accuracy is 97.6%. This accuracy is much higher than that of WiWho [5] (about 80% with 6 subjects) and WifiU [6] (92.31% with 10 subjects and 40 training samples for each subject) which need people to walk along a predefined path for about 5m.

We evaluate the efficiency of RFree-ID on a laptop equipped with an Intel Corei5 CPU running at 2.8 GHz. When the tagret group size is 30 and training set size is 20 for each volunteer, the average computation time to identify an individual is 1.73s. When the target group size is 10, the time decreases to 0.74s. As our system does not need too much real-time quality, this delay is totally acceptable. Actually, we can improve the efficiency via many methods, for example, we can use some pruning algorithms to reduce computation load. To be specific, we first select top k possible candidates using only a few training profiles and then find the final result among these k candidates using all training profiles. In this way, we can reduce the average computation time for identifying an individual to 0.67s with a group size of 30.

5.5. System Resilience to Walking Cofactors Changes

In this section, we test the resilience of our system to walking cofactors changes. The cofactors in our experiments are listed in Table 2. Specifically, we ask volunteers to walk through the sensing area carrying a backpack filled with a laptop, making a phone call, and carrying a laptop, respectively (see Fig. 16). These three manners are very common in home and office settings. It is noted that making phone calls can also change walking patterns because the arm with the phone does not swing as normal walking. As clothes people wear can influence the signal propagation, we also conduct experiments with people wearing winter clothes (the training profiles are collected when people wear spring clothes). In addition, to examine the impact of walking path inconsistency, we ask volunteers to walk along Path2 and Path3 as shown in Fig. 9. We further investigate the robustness of our system to environmental changes by placing a desk nearby and asking another subject to walk around the sensing area. The target group size is 10, and each volunteer walks for 40 times with each cofactor. Fig. 12 is the experimental results. We compare our system with naive MD-DTW method and single tag system. It can be clearly observed that our system outperforms the other two methods significantly in presence of these confounding factors. Specifically, the single tag system yields very poor performance in these scenarios. Naive MD-DTW method incorporates rich spatial

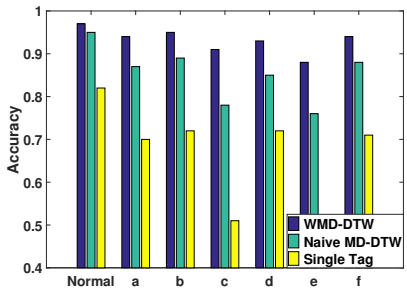

Figure 12: Identification Accuracy VS Cofactors

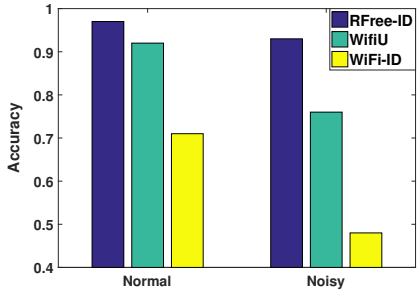

Figure 13: Comparison of RFree-ID with WiFi-based methods

diversity, yet still degrades a lot with cofactor changes. In contrast, the performance of our system does not have obvious degradation and still reaches a high average accuracy of 94.2%, only a slight drop compared to 97.6% in normal walking. This is because our system exploits multiple tags to provide both spatial and temporal walking information, and further highlights the informative signal as well as dampens the noisy signal via the weighting scheme.

5.6. Performance Comparison between RFree-ID and WiFi-based Methods

In this section, we compare our system with recent WiFi-based methods. These WiFi-based work [5][6][31] obtain CSI from WiFi signals to perform human identification. We implement WiFi-ID [31] and WifiU [6] on a laptop equipped with Intel 5300 wireless card. This wireless card can be used to collect CSI measurements[37]. A NetGear R7000 router serves as a signal transmitter. The scenario of WiFi-ID is more similar with ours, where people also walk through the two devices. On the other hand, WifiU requires people to walk along a predefined straight line for more than 5m. We perform the same experiments with the same 10 subjects in last subsection. Fig. 13 depicts the performance of the three methods. As shown, even in the normal walking, our system is appreciably better than the other two. The superiority is much more obvious when the walking cofactor changes (Noisy). In the noisy conditions, the accuracy of WiFi-ID drops to only 48%. WifiU extracts more elaborated features from CSI signals so it can achieve a more robust result, yet still suffers seriously with cofactor changes. Compared with WiFi devices, RFID owns the capability of flexible spatial deployment which provides abundant spatial diversity. We make the full potential of this diversity and thus are more reliable and robust under various conditions.

5.7. System Performance in Realistic Scenarios

To further verify RFree-ID's robustness to individuals' walking pattern changes and applicability in real settings, we perform evaluation in an uncontrolled scenario over a period of three weeks. We deploy our system in the corridor near

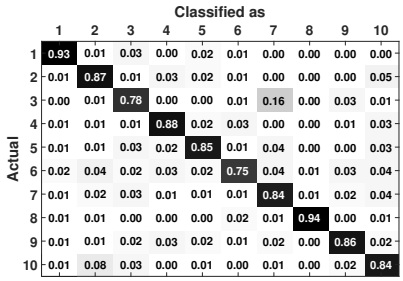

Figure 14: Confusion matrix with naive MD-DTW

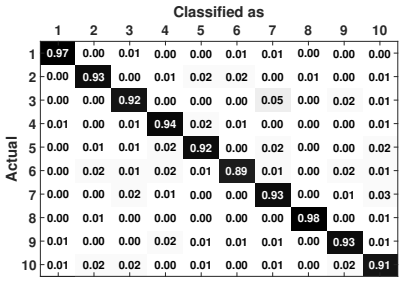

Figure 15: Confusion matrix with WMD-DTW

our lab (as depicted in Fig. 9). As the volunteers participating in the evaluation are students in our lab or other labs in this floor, they walk through the corridor many times nearly every day. To simulate the real world scenarios, we will not give any instructions to them after we collect their training data in normal walking. They can come to or leave their labs as usual and they are free to change their walking pattern as they want. We estimate the ground truth using the camera installed on the ceiling and discard the data collected when more than one person crosses the sensing area at the same time. From the videos, we observe that subjects walk in various patterns. Besides those mentioned above, they may walk through the sensing area looking down at the cellphone, carrying a handbag, in a slow or fast speed, and with or without arm swinging, etc. We collect 1213 walking profiles in total, and more than 80 for each student. We use these walking profiles as testing data and perform evaluation via naive MD-DTW method and our WMD-DTW method, respectively. Fig. 14 and Fig. 15 are the results. The average accuracy is 85.3% and 93.1%, respectively. Specifically, naive MD-DTW method is likely to misclassify subject 3 as subject 7 due to the small discrepancy between their phase profiles. In contrast, our method reduces the misclassification rate from 16% to 5%. This is because we assign higher weights to tags with high distinguishability and lower weights to those with low distinguishability. In addition, subject 6 usually exhibits a significantly different walking pattern (carrying a backpack and with hands in pockets) compared to training process, so his corresponding accuracy is only 75% when using naive MD-DTW method. But our method can boost the accuracy to 89% with the dynamic weighting mechanism. The result indicates that our system has high applicability in real world scenarios.

5.8. Impact of NLOS

In this section, we study the impact of NLOS by placing the reader antenna behind a $120mm$ hollow wall (the wall behind the read antenna in Fig. 9). In this scenario, we collect training samples of normal walking from 10 subjects and use these data to perform cross validation. The average accuracy is 95.4%,

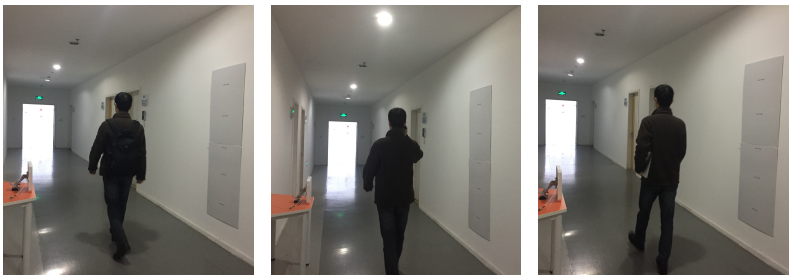

(a) (b) (c)

Figure 16: (a) carrying a backpack; (b) making a phone call; (c) carrying a laptop

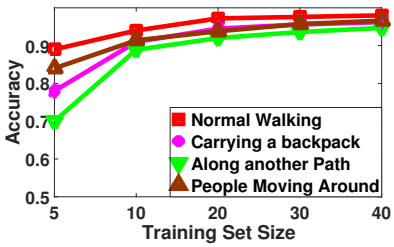

Figure 17: Accuracy VS Training Size

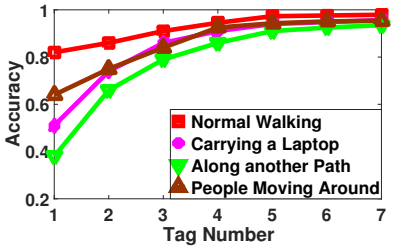

Figure 18: Accuracy VS Tag Number

degrading little compared to LOS scenarios. The result shows that our system works very well in NLOS conditions. This is useful for the deployment in real world scenarios, because in some settings, it may be inappropriate to deploy the reader antenna in the corridor considering such factors as aesthetics, space limitations, or security. Compared to the vision-based techniques which can only work under LOS conditions, our system provides more choice in deployment.

5.9. Impact of Training Set Size

In this section, we evaluate the impact of training set size on the identification result. We consider 4 scenarios including normal walking, carrying a backpack, walking along another path and people moving around. The target group size is 10 (the remaining experiments are all 10). The results are shown in Fig. 17. We observe that a larger training size results in a better result and the performance improvement in latter three scenarios is more remarkable. This is expected because more training instances can yield a more robust result. In addition, our system can exert its superiority better with more samples due to the weighting mechanism. When the size is 20, only a slight performance degradation exists for the latter three scenarios and the degradation almost disappears with a size of 40. Considering the overhead in training and computational load in testing, we set the size to 20 in our experiments. As the accuracy still improves slowly with the size increasing over 20, we can choose a larger size in

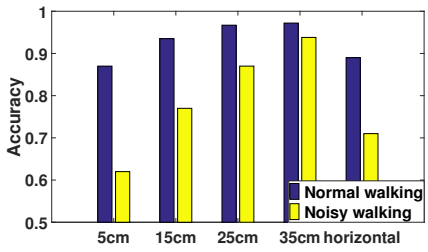

Figure 19: Accuracy VS Tag interval

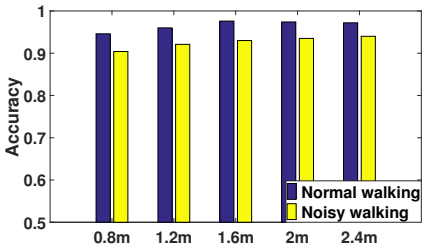

Figure 20: Accuracy VS T-R distance

more noisy conditions.

5.10. Impact of the Number of Tags

As more tags can provide richer spatial and temporal phase measurements for human identification, we study the impact of the number of tags on the performance of our system. The scenarios are the same as Section 5.9. We vary the number of tags from 1 to 7 and show the results in Fig. 18. We can see a similar tendency with Fig. 17. The result strongly indicates that our multiple-tag system can effectively mitigate the effect of walking cofactor changes. RFree-ID finds a trade-off and selects 5 tags in other experiments.

5.11. Impact of Devices Deployment

Tag deployment is crucial to the system performance since it determines the capacity of tags for providing spatial diversity. We deploy 5 tags uniformly in the vertical direction and perform experiments by varying their interval from $5cm$ to $35cm$. Fig. 19 shows the results. Obviously, the accuracy boosts notably with the tag interval increasing, especially for noisy walking (with cofactors variations). This is reasonable since a larger tag interval brings richer spatial diversity. Conversely, with a small interval, tags are more likely to experience similar propagation paths just like multiple subcarriers of WiFi signal or the compact antenna array of WiFi router. When the interval is $35cm$, the distribution range of tags in the vertical direction is $0.4m \sim 1.8m$, which can cover the whole body of almost everyone in our experiments and provide enough spatial diversity. Thus, we set $35cm$ as the interval in other experiments. In addition, we perform experiments when the tags are distributed along the horizontal direction. Similarly, due to the limited spatial diversity, the system performance is much worse than that in the vertical direction.

We further investigate the impact of the horizontal distance between the tag array and the reader antenna (T-R distance). We vary the distance from $0.8m$ to $2.4m$. Fig. 20 depicts the results. We can observe that the accuracy of our system retains high and stable with the distance varying, and can yield 94.6% (normal walking) and 90.4% (noisy walking) even when the distance is only $0.8m$. As the duration of the extracted profiles is only $2.4s$ (Section 4.3)

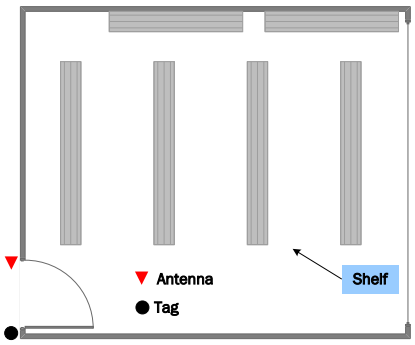

Figure 21: Layout in the workplace library management scenario

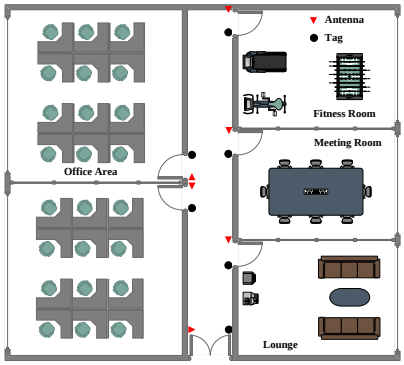

Figure 22: Layout in the room-level tracking scenario

and people's walking speed is about $1m/s$ in normal conditions, our system only need people to walk along a straight line for about $2.5m$. Actually, when the T-R distance is $0.8m$, a straight walkway longer than $1.6m$ is enough. These evaluations allow us to deploy our system to a wide range of application settings, such as a corridor, a narrow or wide entrance in home or office settings.

6. Applications

The design of RFree-ID unlocks a wide range of applications. To demonstrate its practical value, we prototype two applications on top of RFree-ID. In this section, we briefly describe these two prototype applications.

6.1. Workplace library management

User scenario: In the first application, we integrate RFree-ID into the management of tiny workplace libraries. Nowadays, many corporations have their own libraries serving employees [38]. These libraries can be company-wide or just departmental. They can house technical books, leisure reading or other office materials. Having a library at the workplace offers employees opportunities to solve problems and enhance themselves as well as relax outside the work. For the reason of small-scale and saving cost, most libraries in the workplace have no librarians. As a result, employees may forget to return the book they borrow when they finish reading. If other people want to borrow the same book, they don't know who they should find. In our scenario, we enable an automatic book registration system with RFID. First, we leverage RFree-ID to identify the people walking in or out of the library. Then, we pair the people with the book they taking by detecting the signal change of the tag attached on it.

Implementation: We deploy the system into the library of our laboratory where each book is attached on a tag. RFree-ID is deployed near the door, as

Fig. 21 depicts. When RFree-ID identifies the people through the door, the library management system will detect whether they take books with them. As the books on the shlef may also be interrogated by the reader antenna, we differentiate the book people take from them by signal changes of book tags. The signal phase and RSSI in this duration are extracted and denoised. We distill features from them (Section. 4.2) and apply a decision tree classifier to determine the book state. People can take 0/1/2/3 books with them. The system achieves a user-book pairing accuracy of 96.5% to 94.7% with a group size of 10 to 20 people.

6.2. Room-level tracking

User scenario: In the second application, RFree-ID is used as an doorway tracking system to enable individuals' room-level localization. Many indoor environments such as home or workplace are organized into rooms with distinct functionalities. For instance, a typical office workplace consists of offices, meeting rooms, lounges or even fitness rooms. RFree-ID can be deployed near the door of each room to identify employees in/out of the room. A knowledge of employees' room-level location will offer valuable insights on their activities in the workplace. For example, that an employee steps away from the office area and walks into the lounge is likely to mean that he/she breaks up sedentary work to get food or drink, or just have a rest. Researches have shown that adequate work break can reduce an employee's risk of developing chronic conditions as well as improve their wellbeing and productivity [39]. With the help of our system, employees are aware of their physical activities and work break durations so that they can make reasonable adjustment on their time allocation and own more healthy work life.

Implementation: We deploy the tracking system into our lab. The layout is shown in Fig. 22. Two readers and six antennas are used. RFree-ID records crossing events in each door. Instead of only relying on a single doorway crossing, we consider sequences of multiple crossings and perform a joint optimization to track individuals. We integrate RFree-ID with TransTrack [40], a multiple-hypothesis tracking (MHT) method. This can typically correct errors made on a single doorway with subsequent observations made on other doorways. We perform an in-situ experiment for a week with 10 subjects and collect 1067 crossing events. Our tracking system can detect and identify these crossing events with 95.4% accuracy.

7. Discussion and Future Work

7.1. Stranger Detection

RFree-ID focuses on identifying people who has enrolled his/her profiles and does not consider the detection of a stranger who is not in the group. Yet we still make an exploration on stranger detection. As mentioned in Section 4.5, when the WMD-DTW distance is larger than a threshold, it is very likely that the testing profile belongs to a stranger. We use this method to perform stranger

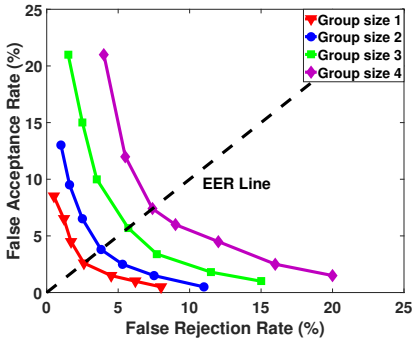

Figure 23: FAR and FRR in normal conditions

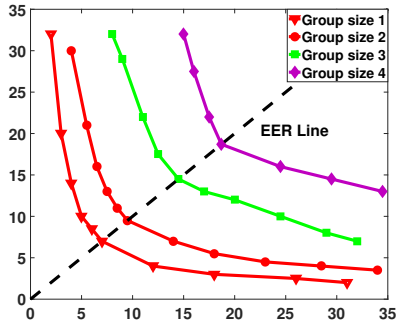

Figure 24: FAR and FRR in noisy conditions

detection and evaluate the identification accuracy in terms of False Acceptance Rate (FAR) and False Rejection Rate (FRR). The FAR is defined as the rate that a stranger is wrongly classified as the subject in the known group and the FRR is the rate that the known subject is wrongly classified as a stranger. Since we can trade off between the FAR and FRR by changing the threshold for identification, we define the Equal Error Rate (EER) point as the point that FAR and FRR are equal. When the walking cofactors are consistence, RFree-ID can achieves an average EER of 7.4% with a group size of 4 (Fig. 23). The result is far better than Rapid (EER, 19.5%) which integrates WiFi with acoustic information [32]. However, when the walking cofactors change, the EER increases to 18.7% (Fig. 24). This is because the influence of the cofactors on walking profiles will make it difficult to judge if a "stranger" is a true stranger or just cofactors distort the profiles of a subject in database. Though our method can mitigate the influence, cofactors changes still lead to non-negligible performance degradation on stranger detection. We may need to deploy more antennas and use other machine learning methods to effectively handle this issue.

7.2. Multiple user scenario

RFree-ID fails to perform identification when there are multiple people walking in the sensing area at the same time. The signal fluctuations captured by RFree-ID under this condition are mixture of multiple walking users and we cannot separate the phase profile of one person from others. Some works have started to explore the detection of multiple people walking together [41]. Based on the occupant number estimation, further signal separation can be explored. Since RFID tags are easy-to-deploy, we plan to deploy more antennas and design more elaborate tag array to perform signal separation when there are multiple walking users.

7.3. Backscatter Sensing

Recently, ambient backscatter communication has been emerging as a promising technology which enables smart devices to communicate by utilizing ambient radio frequency (RF) signals. Researchers developed systems leveraging TV [42], WiFi [43], or even visible light [44] to communicate with battery-free devices. PassiveVLC [44] for example enables a battery-free tag device to perform passive communication with the illuminating LEDs. Compared to RFID, these radios are more pervasive, especially in home settings. There already have works using battery-free WiFi tags for human-object interaction [45]. The idea of RFree-ID also applies to these emerging techniques. In the future, we intend to make an exploration on human identification with ambient backscatter communication.

8. Conclusion

In this paper, we demonstrate the feasibility of exploiting walking-induced RFID signal to enable human identification. We design and implement RFree-ID, an unobtrusive and low-cost yet accurate human identification system with COTS RFID devices. RFree-ID employs multiple spatially distributed tags to obtain the spatial and temporal phase information, and enables human identification via a sequence of signal processing techniques and WMD-DTW algorithm. In contrast to previous radio-based systems which are vulnerable to walking cofactors changes, RFree-ID can effectively handle these variations. Experimental results show that our system is reliable and robust in various conditions. We envision that our system can be an enabling tool for many personalized services in smart buildings and can also effectively facilitate the development of radio-based human sensing techniques.

References

[1] S. Savazzi, S. Sigg, M. Nicoli, V. Rampa, S. Kianoush, U. Spagnolini, Device-free radio vision for assisted living: Leveraging wireless channel quality information for human sensing, IEEE Signal Processing Magazine 33 (2) (2016) 45–58. doi:10.1109/MSP.2015.2496324.

[2] F. Adib, D. Katabi, See through walls with wifi!, in: Proceedings of the ACM SIGCOMM 2013 Conference on SIGCOMM, SIGCOMM '13, ACM, 2013, pp. 75–86. doi:10.1145/2486001.2486039.

[3] K. Joshi, D. Bharadia, M. Kotaru, S. Katti, Wideo: Fine-grained device-free motion tracing using rf backscatter, in: 12th USENIX Symposium on Networked Systems Design and Implementation (NSDI 15), 2015, pp. 189–204.

[4] J. Liu, Y. Wang, Y. Chen, J. Yang, X. Chen, J. Cheng, Tracking vital signs during sleep leveraging off-the-shelf wifi, in: Proceedings of the 16th ACM International Symposium on Mobile Ad Hoc Networking and Computing, ACM, 2015, pp. 267–276. doi:10.1145/2746285.2746303.

[5] Y. Zeng, P. H. Pathak, P. Mohapatra, Wiwho: Wifi-based person identification in smart spaces, in: 2016 15th ACM/IEEE International Conference on Information Processing in Sensor Networks (IPSN), IEEE, 2016, pp. 1–12.

[6] W. Wang, A. X. Liu, M. Shahzad, Gait recognition using wifi signals, in: Proceedings of the 2016 ACM International Joint Conference on Pervasive and Ubiquitous Computing, ACM, 2016, pp. 363–373. doi:10.1145/2971648.2971670.

[7] Q. Zhang, D. Li, R. Zhao, D. Wang, Y. Deng, B. Chen, Rfree-id: An unobtrusive human identification system irrespective of walking cofactors using cots rfid, in: Pervasive Computing and Communications (PerCom), 2018 IEEE International Conference on, IEEE, 2018.

[8] H. Li, C. Ye, A. P. Sample, Idsense: A human object interaction detection system based on passive uhf rfid, in: Proceedings of the 33rd Annual ACM Conference on Human Factors in Computing Systems, ACM, 2015, pp. 2555–2564.

[9] L. Shangguan, Z. Zhou, X. Zheng, L. Yang, Y. Liu, J. Han, Shopminer: Mining customer shopping behavior in physical clothing stores with cots rfid devices, in: Proceedings of the 13th ACM Conference on Embedded Networked Sensor Systems, ACM, 2015, pp. 113–125. doi:10.1145/2809695.2809710.

[10] H. Ding, L. Shangguan, Z. Yang, J. Han, Z. Zhou, P. Yang, W. Xi, J. Zhao, Femo: A platform for free-weight exercise monitoring with rfids, in: Proceedings of the 13th ACM Conference on Embedded Networked Sensor Systems, ACM, 2015, pp. 141–154. doi:10.1145/2809695.2809708.

[11] W. Ruan, L. Yao, Q. Z. Sheng, N. Falkner, X. Li, T. Gu, Tagfall: Towards unobstructive fine-grained fall detection based on uhf passive rfid tags, in: proceedings of the 12th EAI International Conference on Mobile and Ubiquitous Systems: Computing, Networking and Services on 12th EAI International Conference on Mobile and Ubiquitous Systems: Computing, Networking and Services, 2015, pp. 140–149.

[12] L. Yao, Q. Z. Sheng, X. Li, T. Gu, M. Tan, X. Wang, W. Zou, Compressive representation for device-free activity recognition with passive rfid signal strength, IEEE Transactions on Mobile Computing.

[13] C. Shi, J. Liu, H. Liu, Y. Chen, Smart user authentication through actuation of daily activities leveraging wifi-enabled iot, in: Proceedings of the 18th ACM International Symposium on Mobile Ad Hoc Networking and Computing, ACM, 2017, p. 5.

[14] J. Gummeson, J. Mccann, C. J. Yang, D. Ranasinghe, S. Hudson, A. Sample, Rfid light bulb: Enabling ubiquitous deployment of interactive rfid

systems, Proc. ACM Interact. Mob. Wearable Ubiquitous Technol. (2017) 12:1–12:16.

[15] J. Wang, D. Katabi, Dude, where's my card?: Rfid positioning that works with multipath and non-line of sight, ACM SIGCOMM Computer Communication Review 43 (4) (2013) 51–62. doi:10.1145/2486001.2486029.

[16] L. Yang, Y. Chen, X.-Y. Li, C. Xiao, M. Li, Y. Liu, Tagoram: Real-time tracking of mobile rfid tags to high precision using cots devices, in: Proceedings of the 20th annual international conference on Mobile computing and networking, ACM, 2014, pp. 237–248. doi:10.1145/2639108.2639111.

[17] L. Shangguan, K. Jamieson, The design and implementation of a mobile rfid tag sorting robot, in: Proceedings of the 14th Annual International Conference on Mobile Systems, Applications, and Services, ACM, 2016, pp. 31–42. doi:10.1145/2906388.2906417.

[18] A. Jayatilaka, D. C. Ranasinghe, Real-time fluid intake gesture recognition based on batteryless uhf rfid technology, Pervasive and Mobile Computingdoi:http://dx.doi.org/10.1016/j.pmcj.2016.04.007.

[19] Y. Zou, J. Xiao, J. Han, K. Wu, Y. Li, L. M. Ni, Grfid: A device-free gesture recognition system using cots rfid device 16 (2) (2016) 381–393. doi:10.1109/TMC.2016.2549518.

[20] H. Li, E. Brockmeyer, E. J. Carter, J. Fromm, S. E. Hudson, S. N. Patel, A. Sample, Paperid: A technique for drawing functional battery-free wireless interfaces on paper, in: Proceedings of the 2016 CHI Conference on Human Factors in Computing Systems, ACM, 2016, pp. 5885–5896. doi:10.1145/2858036.2858249.

[21] S. Pradhan, E. Chai, K. Sundaresan, L. Qiu, M. A. Khojastepour, S. Rangarajan, Rio: A pervasive rfid-based touch gesture interface, in: Proceedings of the 23rd Annual International Conference on Mobile Computing and Networking, ACM, 2017, pp. 261–274. doi:10.1145/3117811.3117818.

[22] L. Wang, T. Tan, H. Ning, W. Hu, Silhouette analysis-based gait recognition for human identification, IEEE transactions on pattern analysis and machine intelligence 25 (12) (2003) 1505–1518. doi:10.1109/TPAMI.2003.1251144.

[23] C. Wang, J. Zhang, L. Wang, J. Pu, X. Yuan, Human identification using temporal information preserving gait template, IEEE Transactions on Pattern Analysis and Machine Intelligence 34 (11) (2012) 2164–2176. doi:10.1109/TPAMI.2011.260.

[24] H. Lu, J. Huang, T. Saha, L. Nachman, Unobtrusive gait verification for mobile phones, in: Proceedings of the 2014 ACM international symposium on wearable computers, ACM, 2014, pp. 91–98. doi:10.1145/2634317.2642868.

[25] R. San-Segundo, J. D. Echeverry-Correa, C. Salamea-Palacios, S. L. Lutfi, J. M. Pardo, I-vector analysis for gait-based person identification using smartphone inertial signals, Pervasive and Mobile Computingdoi:https://doi.org/10.1016/j.pmcj.2016.09.007.

[26] J. T. Geiger, M. Kneißl, B. W. Schuller, G. Rigoll, Acoustic gait-based person identification using hidden markov models, in: Proceedings of the 2014 Workshop on Mapping Personality Traits Challenge and Workshop, ACM, 2014, pp. 25–30. doi:10.1145/2668024.2668027.

[27] A. Bränzel, C. Holz, D. Hoffmann, D. Schmidt, M. Knaust, P. Lühne, R. Meusel, S. Richter, P. Baudisch, Gravityspace: tracking users and their poses in a smart room using a pressure-sensing floor, in: Proceedings of the SIGCHI Conference on Human Factors in Computing Systems, ACM, 2013, pp. 725–734. doi:10.1145/2470654.2470757.

[28] S. Pan, T. Yu, M. Mirshekari, J. Fagert, A. Bonde, O. J. Mengshoel, H. Y. Noh, P. Zhang, Footprintid: Indoor pedestrian identification through ambient structural vibration sensing, Proceedings of the ACM on Interactive, Mobile, Wearable and Ubiquitous Technologies 1 (3) (2017) 89. doi:10.1145/3130954.

[29] F. H. C. Tivive, A. Bouzerdoum, M. G. Amin, A human gait classification method based on radar doppler spectrograms, EURASIP Journal on Advances in Signal Processing 2010 (1) (2010) 1. doi:10.1155/2010/389716.

[30] F. Adib, C.-Y. Hsu, H. Mao, D. Katabi, F. Durand, Capturing the human figure through a wall, ACM Transactions on Graphics (TOG) 34 (6) (2015) 219. doi:10.1145/2816795.2818072.

[31] J. Zhang, B. Wei, W. Hu, S. Kenhere, Wifi-id: Human identification using wifi signal, in: 2016 International Conference on Distributed Computing in Sensor Systems (DCOSS), 2016, pp. 75–82. doi:10.1109/DCOSS.2016.30.

[32] Y. Chen, W. Dong, Y. Gao, X. Liu, T. Gu, Rapid: A multimodal and device-free approach using noise estimation for robust person identification, Proc. ACM Interact. Mob. Wearable Ubiquitous Technol. 41:1–41:27doi:10.1145/3130906.

[33] Impinj, Speedway revolution reader application note - low level user data support (2013).

[34] D. M. Dobkin, The rf in RFID: uhf RFID in practice, Newnes, 2012.

[35] S. Tan, J. Yang, Wifinger: leveraging commodity wifi for fine-grained finger gesture recognition, in: Proceedings of the 17th ACM International Symposium on Mobile Ad Hoc Networking and Computing, ACM, 2016, pp. 201–210. doi:10.1145/2942358.2942393.

[36] Y.-S. Jeong, M. K. Jeong, O. A. Omitaomu, Weighted dynamic time warping for time series classification, Pattern Recognition 44 (9) (2011) 2231–2240.

[37] D. Halperin, W. Hu, A. Sheth, D. Wetherall, Tool release: Gathering 802.11 n traces with channel state information, ACM SIGCOMM Computer Communication Review 41 (1) (2011) 53–53.

[38] A. Black, H. Gabb, The value proposition of the corporate library, past and present, Information & Culture 51 (2) (2016) 192–225.

[39] S. A. Cambo, D. Avrahami, M. L. Lee, Breaksense: Combining physiological and location sensing to promote mobility during work-breaks, in: Proceedings of the 2017 CHI Conference on Human Factors in Computing Systems, ACM, 2017, pp. 3595–3607.

[40] A. Kalyanaraman, E. Griffiths, K. Whitehouse, Transtrack: Tracking multiple targets by sensing their zone transitions, in: Distributed Computing in Sensor Systems (DCOSS), 2016 International Conference on, IEEE, 2016, pp. 59–66.

[41] X. Guo, B. Liu, C. Shi, H. Liu, Y. Chen, M. C. Chuah, Wifi-enabled smart human dynamics monitoring, in: Proceedings of the 15th ACM Conference on Embedded Network Sensor Systems, ACM, 2017. doi:10.1145/3131672.3131692.

[42] V. Liu, A. Parks, V. Talla, S. Gollakota, D. Wetherall, J. R. Smith, Ambient backscatter: wireless communication out of thin air, in: ACM SIGCOMM Computer Communication Review, Vol. 43, ACM, 2013, pp. 39–50.

[43] B. Kellogg, V. Talla, S. Gollakota, J. R. Smith, Passive wi-fi: Bringing low power to wi-fi transmissions., in: NSDI, Vol. 16, 2016, pp. 151–164.

[44] X. Xu, Y. Shen, J. Yang, C. Xu, G. Shen, G. Chen, Y. Ni, Passivevlc: Enabling practical visible light backscatter communication for battery-free iot applications, in: Proceedings of the 23rd Annual International Conference on Mobile Computing and Networking, ACM, 2017, pp. 180–192.

[45] C. Gao, Y. Li, X. Zhang, Livetag: Sensing human-object interaction through passive chipless wifi tags, in: 15th USENIX Symposium on Networked Systems Design and Implementation (NSDI 18), USENIX, 2018.